NANO LETTERS

2006
Vol. 6, No. 5
1007−1012

Patterning Polyethylene Oligomers on Carbon Nanotubes Using Physical Vapor Deposition

Lingyu Li,[†] Yao Yang,[‡] Guoliang Yang,[‡] Xuming Chen,[§] Benjamin S. Hsiao,[§] Benjamin Chu,[§] Jonathan E. Spanier,[†] and Christopher Y. Li*,[†]

A. J. Drexel Nanotechnology Institute and Department of Materials Science and Engineering, Drexel University, Philadelphia, Pennsylvania 19104, Department of Physics, Drexel University, Philadelphia, Pennsylvania 19104, and Department of Chemistry, Stony Brook University, Stony Brook, New York 11794

Received February 6, 2006; Revised Manuscript Received March 26, 2006

ABSTRACT

Periodic patterning on one-dimensional (1D) carbon nanotubes (CNTs) is of great interest from both scientific and technological points of view. In this letter, we report using a facile physical vapor deposition method to achieve periodic polyethylene (PE) oligomer patterning on individual CNTs. Upon heating under vacuum, PE degraded into oligomers and crystallized into rod-shaped single crystals. These PE rods periodically decorate on CNTs with their long axes perpendicular to the CNT axes. The formation mechanism was attributed to "soft epitaxy" growth of PE oligomer crystals on CNTs. Both SWNTs and MWNTs were decorated successfully with PE rods. The intermediate state of this hybrid structure, MWNTs absorbed with a thin layer of PE, was captured successfully by depositing PE vapor on MWNTs detached from the solid substrate, and was observed using high-resolution transmission electron microscopy. Furthermore, this hybrid structure formation depends critically on CNT surface chemistry: alkane-modification of the MWNT surface prohibited the PE single-crystal growth on the CNTs. We anticipate that this work could open a gateway for creating complex CNT-based nanoarchitectures for nanodevice applications.

Introduction. Periodic patterning on one-dimensional (1D) carbon nanotubes (CNTs) is of great interest from both scientific and technological points of view. Periodically patterned CNTs could lead directly to controlled two-dimensional (2D) or three-dimensional (3D) CNT suprastructures, an essential step toward building future CNT-based nanodevices. Although both chemical and noncovalent CNT functionalization have attracted extensive attention during the past decades,[1−4] very few efforts have been dedicated to periodically patterning on individual CNTs. Czerw et al. demonstrated regular organization of poly(propionylethylenimine-*co*-ethylenimine) (PPEI-EI) on CNTs using scanning tunneling microscopy (STM).[5] CNT electronic structure change upon attachment of polymers was also reported.[6,7] Single-stranded DNA (ssDNA) and proteins have been bound to CNTs, resulting in periodic helical wrapping on the surface of CNTs.[8−10] Helical wrapping SWNT with starch has also been reported.[11,12] Periodic patterning of functionalized SWNTs using Bingle reaction was examined by Worsley et al. using STM, and the occurrence of highly regular (periodicity ∼4.6 nm), long-range patterns was attributed to spatial fluctuation of electron density induced long-range reactivity.[13] Recently, we reported using a controlled polymer solution crystallization method to achieve periodically decorated CNTs and CNFs.[14,15] Polyethylene (PE) and Nylon 6,6 single crystals were controlled to grow on CNTs, forming a unique nanohybrid shish kebab (NHSK) structure. In a NHSK, polymer single crystals are periodically strung along the CNT axis; CNT forms the "shish" while polymer single crystals form the "kebabs". Periodicity can be controlled easily by tuning crystallization conditions. In a solution-formed NHSK, the 2D lamellar (kebab) normal is parallel to the 1D tubes, rendering a 3D nature of the NHSK. The 3D structure is advantageous for a number of applications such as nanocomposites. In other fields such as nanoelectronics, however, a 2D hybrid structure is preferred, which demands the need for an alternative means for fabricating periodic patterns on CNTs.

The physical vapor deposition (PVD) technique is used widely for solid surface study. Upon heating under vacuum, metals/polymers decompose into small particles/oligomers and deposit on solid surfaces.[16−24] Gold has long been used as the evaporation source to decorate polymer surfaces to reveal fine surface topography.[16,17] PE has also been used

* To whom correspondence should be addressed. E-mail: chrisli@drexel.edu. Tel: 215-895-2083. Fax: 215-895-6760.
[†] A. J. Drexel Nanotechnology Institute and Department of Materials Science and Engineering, Drexel University.
[‡] Department of Physics, Drexel University.
[§] Stony Brook University.

10.1021/nl060276q CCC: $33.50
Published on Web 04/26/2006

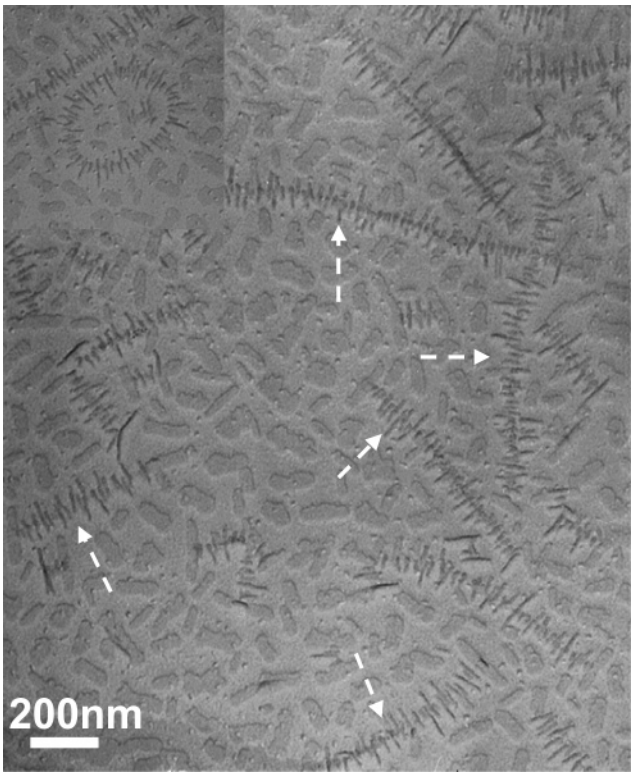

Figure 1. TEM image of PE-decorated SWNTs. Arrows indicate "nanocentipede-like" 2D nanostructures, which are named 2D nanohybrid shish kebabs. SWNTs form the central shish (the "body of the centipede") and PE rods form the kebabs ("centipede" feet). PE crystalline rods are perpendicular to the SWNT axes. The inset shows a "nanonecklace" formed by PE decorating on a SWNT loop. Note that PE rods are locally perpendicular to the SWNT axis.

to investigate polymer surfaces.[18,19,21−24] Upon heating under vacuum, PE degrades into oligomers that form rod-shaped single crystals. The orientation of the rods is particularly sensitive to the substrate surface feature. Polymer single-crystal sectorization and chain folding have been investigated successfully using this technique.[18,19,21−24]

In this letter, we report using the polymer PVD method as a facile means to achieve periodic patterning on individual CNTs. PE was used as the model compound. The PE single-crystal rods generated during PVD were patterned uniformly on CNTs with the rod long axes being perpendicular to the CNT axis. These rods also relatively periodically span along the entire CNTs. The formation mechanism, generality of the techniques, and the CNT surface chemistry effect were investigated. We anticipate that this work could open a gateway for creating complex CNT-based nanoarchitectures for nanodevice applications.

Results and Discussion. Single-walled carbon nanotube (SWNT)/dichlorobenzene (DCB) solution was first spin-coated on a carbon-coated glass slide and decorated with PE using the PVD method. The detailed experimental procedure can be found in the Supporting Information (Figure S1). Figure 1 shows a transmission electron microscopy (TEM) micrograph of a PE-coated film. The sample was shadowed with a thin layer of Pt/Pd to enhance the contrast. Many small "islands" with an average height of ∼10 nm can be seen on the substrate (the height was estimated using the shadowing angle; it can also be confirmed by AFM experiments, see the following section). Of interest is that numerous "centipede-like" objects can be seen from the image, as indicated by the arrows. Careful examination of the image shows that these "centipedes" are PE-coated SWNTs (or small SWNT bundles): the SWNTs seemingly form the "body of the centipedes" while PE forms the "feet". These "feet" are rod-shaped objects (about 120 nm in length and 10 nm in width). Unlike the rest of the PE "islands" formed on the carbon film, PE rods attaching to SWNTs show uniform orientation and their long axes are perpendicular to the SWNT axes. This peculiar morphology resembles the NHSK we reported recently on the solution-crystallized PE/SWNT hybrid structure. One obvious difference is that NHSK formed in solution crystallization is 3D in nature as discussed previously, while in the present case, both PE rods and SWNTs are 1D objects and the resulting centipede-like hybrid structure is two-dimensional. 2D-NHSK was thus adopted to name this unique structure. CNTs form the shish while PE rods form the kebabs. Compared to solution-formed NHSK, these 2D structures might be more suitable for thin-film nanodevice applications.

The formation mechanism of these 2D NHSK is intriguing. In PVD, PE chain scission occurs upon heating under vacuum (typically $10^{-4}-10^{-5}$ Torr) and the resulting vaporized materials have a molecular weight (MW) on the order of 1300 g/mol.[19,25] Upon deposition on the solid surface, these PE oligomers crystallize, resulting in the rod-shaped objects mentioned previously, which are extended-chain PE crystals with the PE axis being perpendicular to the rod long axis. Each PE rod has a width of about 10 nm, which corresponds to MW of ∼1300 g/mol provided the extended-chain configuration. Most importantly, those PE crystal rods relatively periodically arrange on individual SWNTs and have a periodicity of $\sim 37.4 \pm 7.9$ nm. A histogram of the 2D NHSK periodicity is shown in Figure S2 in the Supporting Information. Although a few of PE nanorods are slightly oblique from the axis normal, most rods are perpendicular to the SWNT axis. The inset of Figure 1 shows a TEM image of a "nanonecklace" structure formed by PE decoration on a SWNT loop. Although the SWNT possesses an eclipse shape with a long axis of ∼200 nm and a short axis of ∼110 nm, rod-shaped PE crystals formed on the SWNT loop as well with their long axes locally perpendicular to the SWNT axis. This suggests that the present PVD method can be adapted for patterning on complex CNT arrays, and the orientation of PE rods is determined by the local CNT axis direction.

The 2D NHSK feature can be confirmed by atomic force microscopy (AFM) experiments. Figure 2 shows the AFM tapping-mode images of PE decoration on SWNTs. Scans [5 μm (a) and 2.5 μm (b)] show that the surface of PE-decorated SWNTs is flat. PE decoration is uniform, and all of the SWNTs are decorated with PE crystal rods. Figures 2c, d, and f are 1 μm scan of the height, amplitude, and top-view images. PE rods relatively periodically span along SWNT. An AFM height profile along the SWNT is shown in Figure 2e. The average height measured from three

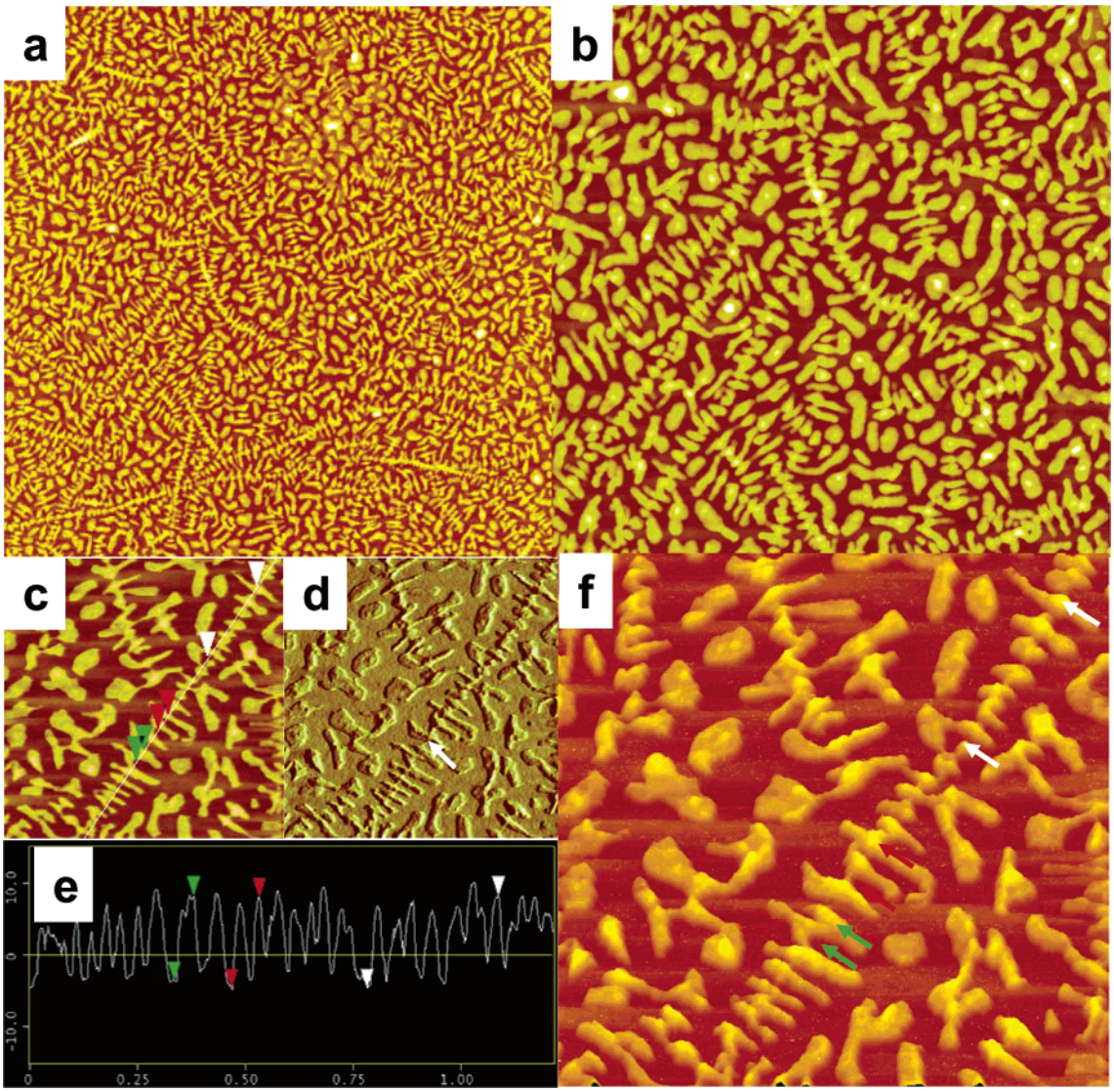

Figure 2. AFM tapping-mode images of the PE-decorated SWNTs. a and b are height images of the 5 μm and 2.5 μm scan, respectively. c, d, and f are the height, amplitude, and top-view images of the 1 μm scan, respectively. e shows a height profile of the 2D NHSK along the SWNT axis.

different spots on one PE-decorated SWNT (indicated by green, red, and white arrows in Figure 2e and f) is 12.4 nm, whereas the PE rods slightly off the 2D-NHSK center have an average height of 10 nm (Supporting Information Figure S3). This suggests that the SWNT possesses a diameter of 2.4 nm. Directly measuring the SWNT height in the interval regions of the PE rods (see Supporting Information Figure S4 for details) also confirms this result. The relatively large diameter indicates small SWNT bundle formation (2−4 SWNTs for each bundle), which is not surprising because aggregation of SWNTs in the present case is dictated by the degree of exfoliation of SWNTs in DCB (more concentrated SWNT solution tends to induce more/larger SWNT bundles). It should be noted that ridges between SWNTs in a bundle might facilitate the PE rod single-crystal growth. Nevertheless, 2D-NHSK can also be formed on single SWNTs as shown in the lower-left corner of Figure 2c. The AFM height profile indicates that the tube diameter is ∼1.2 nm (see Supporting Information Figure S4), indicating the absence of SWNT agglomeration. Hence, formation of the 2D-NHSK is not significantly affected by SWNT aggregation. In all of these images, PE rods were formed on the top of these SWNTs (bundles) and were orthogonally oriented with respect to the tube axis.

The orientation of the PE rods obtained in PVD has been used as a marker to determine the chain-folding direction in polymer single crystals.[19,22,24] In the present case, orthogonal orientation of the rods and CNTs suggests that most of the PE oligomers are parallel to the CNT surface. Previous study showed that PE can epitaxially grow on graphite surfaces, the (110) plane of orthorhombic PE crystals grew parallel to the graphite substrate. The chain axis directions orientated in the ⟨11−20⟩ directions of the graphite surface layer.[26−32] In the present case, however, we observed that PE rods are dominantly perpendicular to the CNT axis. Because the HiPco SWNT was used in this study and a variety of chiral configurations exists in these SWNTs,[33,34] the uniform PE orientation suggests that epitaxy is not the determining factor

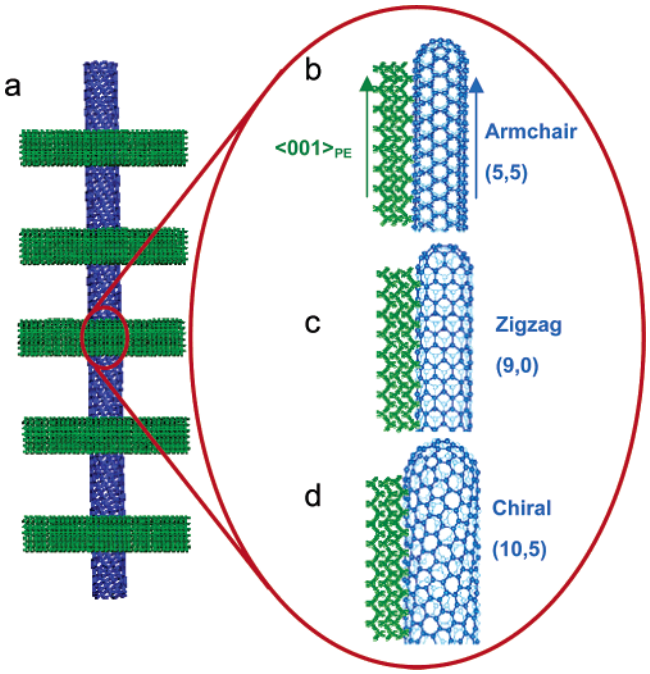

Figure 3. (a) Schematic representation of the 2D NHSK. A SWNT forms the central stem (shish). PE forms elongated, extended-chain single crystals. PE chain axes are perpendicular to the PE rod crystals, while they are also parallel to the SWNT axis. b, c, and d show the PE chain orientation on CNTs with different chirality. No matter whether the CNT possesses an armchair (b), a zigzag (c), or a chiral configuration, PE chains are always parallel to the CNT axis, suggesting a soft epitaxy growth mechanism.

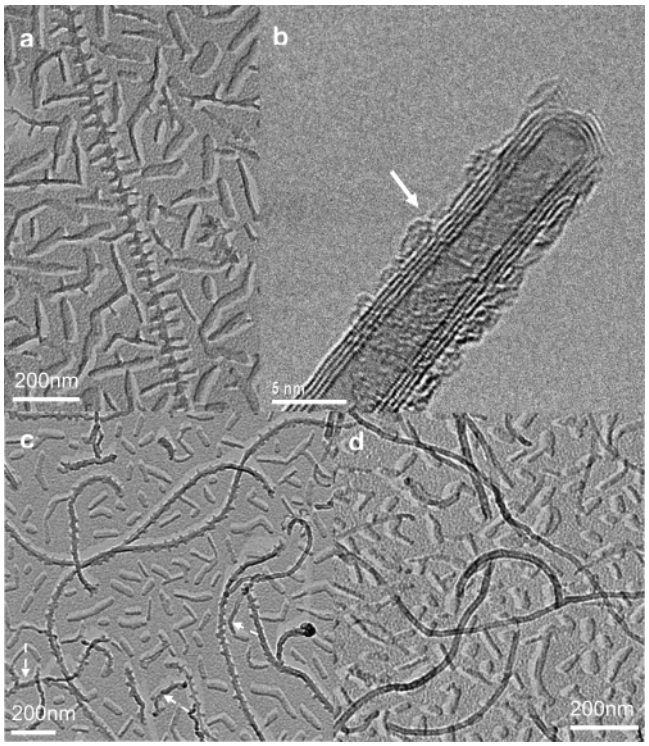

Figure 4. (a) TEM image of PE-decorated AD-MWNTs. b shows an HRTEM image of a PE-decorated AD-MWNT. The MWNT was located in the hole region of a lacey carbon grid. This image captured the intermediate state of the PE decoration process. A thin layer of PE molecules were deposited on the MWNT surface. PE crystals did not grow on the CNT because the MWNT was detached from the substrate; diffusion of PE oligomers onto the CNT surface was thus prohibited. c and d show TEM images of PE decorated on CVD-MWNT (c) and C18-MWNT (d). Lack of PE crystals on the MWNT in d suggests that alkane modification prohibits PE crystal growth on MWNTs, indicating that CNT surface chemistry plays a crucial role in the 2D NHSK formation process.

for PE orientation. This might be due to the small diameter of the SWNTs: because the diameter of the CNTs is small, there are two factors determining PE chain orientation: epitaxy and geometry effect. Epitaxy requires a $\langle 001 \rangle_{PE}$// $\langle 11\text{-}20 \rangle_{graphite}$ orientation. For CNTs with different chirality, following strict epitaxy, PE chain should have different orientations (parallel or oblique to the tube axis). However, because SWNT possesses an extremely small diameter and the tube surface is thus curvy, geometry effect requires the PE chain to be parallel with SWNT axis disregarding the SWNT chirality.[15] Observation of the exclusive orthogonal orientation between SWNT and PE rods suggests that geometry effect plays the major role in determining PE chain orientation. Because strict lattice matching is not required, we name this growth mechanism soft epitaxy. Figure 3 shows the schematics of the 2D NHSK structure. In armchair, zigzag, and chiral SWNTs, $\langle 001 \rangle_{PE}$ or PE chain orientation is always parallel to the SWNT axis. This soft epitaxy mechanism also holds in the case of multiwalled carbon nanotubes (MWNTs). Figure 4a is a TEM image of PE decoration on a MWNT [synthesized by arc discharge method (AD-MWNT), diameter ~5−15 nm]. The morphology is similar to that of a SWNT, indicating that PVD is a generic method for different CNTs.

Because the rods in 2D NHSK are PE oligomer crystals, we anticipate that two steps are involved in the 2D NHSK formation process. In the first step, decomposed PE oligomers (MW ~1300 g/mol) deposit on the solid surface, forming a thin layer on the substrate. During this step, PE oligomers coat the substrate uniformly regardless of the surface chemistry. In the second step, these oligomers self-organize to form single crystals. If the substrate is amorphous carbon, then random orientation of PE crystals is formed. In the CNT case, however, CNT could serve as the nucleation sites. Nuclei formed on CNT and PE oligomers diffuse/crystallize upon these nuclei. The orientation of the nuclei dictates the final orthogonal orientation between PE rods and the CNT axis. Hence, the second step clearly involves surface diffusion and crystallization. To prove this two-step formation hypothesis, we design an experiment to decouple these two steps by using a lacey carbon grid as the substrate to conduct the PVD experiment. A lacey carbon grid consists of a "broken" amorphous carbon film with numerous "holes" (~3−5 μm) to allow high-resolution TEM (HRTEM) observation. By decorating PE on CNT-coated lacey carbon grids, because some of the CNTs dangle on the "holes" and thus are detached from the solid surface, PE oligomers cannot diffuse onto these CNTs to grow further into single crystals. Therefore, for all of the CNTs dangling on the "holes" of lacey carbon grids, 2D NHSK should not form. Indeed, 2D NHSK was not observed in the "hole" region of the grids, and Figure 4b shows an HRTEM image of such a MWNT.

Three layers of the graphene sheets form the MWNT wall and on the MWNT surface, a layer of PE coating can be seen clearly as indicated by the arrows. The PE coating appears to be continuous and has an average thickness of about ~1−2 nm. This continuous PE coating appears to be formed at the very beginning of this PVD process (step 1). Because CNTs are detached from the substrate, PE oligomers could not diffuse and grow further on the CNT surface. The PE oligomers already absorbed on the CNTs in step 1 also could not diffuse away from the CNT surface. The present image therefore captured the intermediate state of the 2D NHSK formation process. On the continuous carbon film area of this grid, the second step is allowed; hence, 2D NHSK structures were formed (Supporting Information Figure S5). The two-step formation mechanism can therefore be confirmed.

Because the formation of the 2D NHSK was due to the nucleation of PE on the CNT surface, the structure and surface chemistry of the CNT might be major factors for PE crystal growth and preferred side-wall structure might be needed. To prove this hypothesis, MWNTs synthesized by the chemical vapor deposition (CVD) method was used in the PE decoration study. Figure 4c shows a TEM image of PE-decorated CVD-MWNTs. PE crystal rods also periodically decorated on MWNTs although they are not as uniform as those on the AD-MWNTs. In some areas, MWNTs were only partially decorated as indicated by the white arrows. This might be due to the defect groups on the CVD-MWNT side walls. To further vary CNT wall structure, octadecylamine was covalently attached to the CVD-MWNT surface as reported (C18-MWNT; details about surface modification can be found in the Supporting Information and references therein). Figure 4d shows the TEM image of PE-decorated C18-MWNTs. It can be seen clearly that while the tubes are curvy, similar to Figure 4c, the CNT surfaces are smooth and PE crystals did not form on the C18-MWNT surface. PE rod crystals formed on the free carbon surface. This indicates clearly that alkane-modified CNTs prohibit PE crystal growth on the CNT surface. It can therefore be concluded that the side-wall structure and surface chemistry of CNTs play a crucial role for successful PE decoration on CNTs. A uniform, smooth graphene-like surface is preferred for PE crystal formation.

Conclusions. In summary, we have shown that, for the first time, the PVD technique could be used for patterning polyethylene oligomers on CNTs. PE was decorated on the surface of SWNTs and MWNTs due to CNT initiated PE crystallization and the 2D NHSK was formed. The orthogonal orientation of the PE rods and the CNT axis was attributed to soft epitaxy. A two-step formation mechanism of the 2D NHSK was proposed and testified by carefully designed HRTEM experiments. CNT side-wall structures and surface chemistry are determining factors for this hybrid structure formation. The reported method possesses the following advantages in forming patterned CNTs: (1) the patterning is on individual CNTs and it is relatively periodic; (2) the PVD process does not involve any solvent and is conducted at room temperature. It can therefore be considered as a green and facile functionalization method; (3) the resulting 2D NHSK could be adapted to create CNT-based nanodevices. Further researches on using different polymers as well as other 1D nanotubes/nanowires are underway.

Acknowledgment. This work was supported by the NSF CAREER award (DMR-0239415), DMI-0508407, 3M, and DuPont.

Supporting Information Available: Experimental section, surface functionalization of CVD-MWNTs. This material is available free of charge via the Internet at http://pubs.acs.org.

References

(1) Chen, J.; Hamon, M. A.; Hu, H.; Chen, Y. S.; Rao, A. M.; Eklund, P. C.; Haddon, R. C. *Science* **1998**, *282*, 95−98.
(2) Hirsch, A. *Angew. Chem., Int. Ed.* **2002**, *41*, 1853−1859.
(3) Sun, Y.; Fu, K.; Lin, Y.; Huang, W. *Acc. Chem. Res.* **2002**, *35*, 1096−1104.
(4) Banerjee, S.; Hemraj-Benny, T.; Wong, S. S. *Adv. Mater.* **2005**, *17*, 17−29.
(5) Czerw, R.; Guo, Z. X.; Ajayan, P. M.; Sun, Y. P.; Carroll, D. L. *Nano Lett.* **2001**, *1*, 423−427.
(6) Bekyarova, E.; Itkis, M. E.; Cabrera, N.; Zhao, B.; Yu, A. P.; Gao, J. B.; Haddon, R. C. *J. Am. Chem. Soc.* **2005**, *127*, 5990−5995.
(7) Balasubramanian, K.; Friedrich, M.; Jiang, C. Y.; Fan, Y. W.; Mews, A.; Burghard, M.; Kern, K. *Adv. Mater.* **2003**, *15*, 1515−1518.
(8) Balavoine, F.; Schultz, P.; Richard, C.; Mallouh, V.; Ebbesen, T. W.; Mioskowski, C. *Angew. Chem., Int. Ed.* **1999**, *38*, 1912−1915.
(9) Zheng, M.; Jagota, A.; Strano, M. S.; Santos, A. P.; Barone, P.; Chou, S. G.; Diner, B. A.; Dresselhaus, M. S.; McLean, R. S.; Onoa, G. B.; Samsonidze, G. G.; Semke, E. D.; Usrey, M.; Walls, D. J. *Science* **2003**, *302*, 1545−1548.
(10) Heller, A. A.; Jeng, E. S.; Yeung, T. K.; Martinez, B. M.; Moll, A. E.; Gastala, J. B.; Strano, M. S. *Science* **2006**, *311*, 508−511.
(11) Star, A.; Stwuerman, D. W.; Heath, J. R.; Stoddart, J. F. *Angew. Chem., Int. Ed.* **2002**, *41*, 2508−2512.
(12) Kim, O. K.; Je, J.; Baldwin, J. W.; Kool, S.; Pehrsson, P. E.; Buckley, L. J. *J. Am. Chem. Soc.* **2002**, *125*, 4426−4427.
(13) Worsley, K. A.; Moonoosawmy, K. R.; Kruse, P. *Nano Lett.* **2004**, *4*, 1541−1546.
(14) Li, C. Y.; Li, L.; Cai, W.; Kodjie, S. L.; Tenneti, K. K. *Adv. Mater.* **2005**, *17*, 1198−1202.
(15) Li, L.; Li, C. Y.; Ni, C. *J. Am. Chem. Soc.* **2006**, *128*, 1692−1699.
(16) Bassett, G. A. *Philos. Magn.* **1958**, *3*, 1042−1045.
(17) Bassett, G. A.; Blundell, D. J.; Keller, A. *J. Macro. Sci. Phys.* **1967**, *B1*, 161−184.
(18) Wittmann, J. C.; Lotz, B. *Makromol. Chem., Rapid Commun.* **1982**, *3*, 733−738.
(19) Wittmann, J. C.; Lotz, B. *J. Polym. Sci., Polym. Phys. Ed.* **1985**, *23*, 205−226.
(20) Wittmann, J. C.; Lotz, B. *J. Mater. Sci.* **1986**, *21*, 659−668.
(21) Li, C. Y.; Yan, D. H.; Cheng, S. Z. D.; Bai, F.; He, T. B.; Chien, L. C.; Harris, F. W.; Lotz, B. *Macromolecules* **1999**, *32*, 524−527.
(22) Li, C. Y.; Cheng, S. Z. D.; Ge, J. J.; Bai, F.; Zhang, J. Z.; Mann, I. K.; Harris, F. W.; Chien, L. C.; Yan, D. H.; He, T. B.; Lotz, B. *Phys. Rev. Lett.* **1999**, *83*, 4558−4561.
(23) Li, C. Y.; Cheng, S. Z. D.; Ge, J. J.; Bai, F.; Zhang, J. Z.; Mann, I. K.; Chien, L. C.; Harris, F. W.; Lotz, B. *J. Am. Chem. Soc.* **2000**, *122*, 72−79.
(24) Li, C. Y.; Ge, J. J.; Bai, F.; Calhoun, B. H.; Harris, F. W.; Cheng, S. Z. D.; Chien, L. C.; Lotz, B.; Keith, H. D. *Macromolecules* **2001**, *34*, 3634−3641.
(25) Satou, M.; Watanabe, Y.; Hayashi, H. *J. Polym. Sci., Part A-2* **1972**, *10*, 835−845.
(26) Tuinstra, F.; Baer, E. *Polym. Lett.* **1970**, *8*, 861−865.
(27) Baukema, P. R.; Hopfinger, A. J. *J. Polym. Sci., Polym. Phys. Ed.* **1982**, *20*, 399−4−9.
(28) Tracz, A.; Jeszka, J.; Kucinska, I.; Chapel, J. P.; Boiteux, G. *Macromol. Symp.* **2001**, *169*, 129−135.

(29) Tracz, A.; Jeszka, J. K.; Kucinska, I.; Chapel, J. P.; Boiteux, G.; Kryszewski, M. *J. Appl. Polym. Sci.* **2002**, *86*, 1329−1336.
(30) Tracz, A.; Kucinska, I.; Jeszka, J. K. *Macromolecules* **2003**, *36*, 10130−10132.
(31) Takenaka, Y.; Miyaji, H.; Hoshino, A.; Tracz, A.; Jeszka, J. K.; Kucinska, I. *Macromolecules* **2004**, *37*, 9667−9669.
(32) Tracz, A.; Ungar, G. *Macromolecules* **2005**, *38*, 4962−4965.
(33) Saito, R.; Dresselhaus, G.; Dresselhaus, M. S. *Physical Properties of Carbon Nanotubes*; Imperial College Press: London, 1998.
(34) Harris, P. J. F. *Carbon Nanotubes and Related Structures*; Cambridge University Press: Cambridge, 1999.

NL060276Q